CHARACTERISTICS OF VORTEX PACKETS IN WALL TURBULENCE

Christopher D. Tomkins
Ronald J. Adrian

Department of Theoretical and Applied Mechanics
University of Illinois at Urbana-Champaign
Urbana, IL 61801, USA

ABSTRACT

Large-scale motions are studied in a $Re_\theta \approx 7700$ turbulent boundary layer using 2-D PIV measurements in the streamwise-spanwise plane. It is known that inclined low momentum regions grow from the wall at this Reynolds number, extending over 2 δ in x and out to 0.8 δ in y, and evidence suggests these structures are induced by packets of hairpin-like vortices aligned in the streamwise direction. The current experiment is designed to investigate the characteristics of these structures. It uses a horizontal plane at $y/\delta = 0.2$ to intersect mature motions and a wide field of view, permitting observation of several large-scale motions on a single realization while adequately resolving the individual structures associated with these motions. Data reveals large-scale low momentum regions elongated in the streamwise direction, bordered by rotating velocity vector patterns and vorticity, suggesting the presence of hairpin or cane-like vortices. Characteristics of these large-scale motions are investigated, including streamwise and spanwise size, shape, and spanwise spacing. Characteristics of the associated hairpin vortex packets investigated include number of vortices, streamwise alignment, and the nature, size, and symmetry of individual member vortices.

INTRODUCTION

Understanding mass and momentum transport mechanisms towards and away from the wall is an important step in understanding wall turbulence. One important and frequently observed mechanism by which this transport may occur is the inclined hairpin-like vortex. Groups of such structures have been measured in both low Reynolds number wall layers (Smith, 1984) and outer regions of high Reynolds number wall layers (Head and Bandyopadhyay, 1981). Recent particle image velocimetry (PIV) measurements in the streamwise-wall-normal (x-y) plane of a turbulent boundary layer suggest that these vortices organize in the streamwise direction to form coherent groups or packets extending throughout the boundary layer at both high and low Reynolds number (Meinhart et al., 1999; Tomkins et al., 1998; Tomkins, 1997; Meinhart and Adrian, 1996). These vortex packets appear to work cooperatively to induce a large low-momentum region of much greater extent than an individual vortex. The low-momentum regions are typically angled upward from the wall between 10 and 20 degrees, and may extend over 2 δ streamwise and out to 0.8 δ in the wall-normal direction. Hence, these regions are quite distinct from the low speed streaks observed in the near-wall region by Kline (1967) and others. Packets have been observed containing up to 9 vortices. The organization of vortices into packets and the possible interaction of those packets provides a new paradigm by which many frequently observed but seemingly unconnected aspects of wall turbulence can be explained. This hairpin vortex packet paradigm also presents the interesting idea that transport properties of the packet could significantly exceed the sum of the individual vortices, and thus presents potentially interesting implications for issues such as drag reduction.

However, while the implications of these ideas are readily understood, several important questions remain concerning the 3-dimensional characteristics of the structures themselves. In particular, it is unresolved whether or not measurements providing spanwise information are completely consistent with the above observations. Also unknown are the 3-dimensional characteristics of the individual vortex structures in these packets, and the 3-D characteristics of the packets/low-momentum regions themselves. A final unknown is the spanwise spacing of these large-scale motions, including the potential for packet-packet spanwise interaction. While previous studies in the horizontal plane exist (Lui et al., 1996), measurements were made in a lower Reynolds number channel flow closer to the wall. The channel half-height in terms of inner units was $h^+ = 395$, thus limiting the potential growth of these structures, which in this boundary layer commonly reach $y^+ = 1100$.

The present work involves PIV measurements in the streamwise-spanwise plane of a zero-pressure gradient flat plate turbulent boundary layer with the goal of resolving several of these currently unresolved issues. The data set in this paper includes measurements at $y/\delta = 0.2$ in a moderately high ($Re_\theta \approx 7700$) flow. The height is chosen so the measurement volume intersects the mature large-scale structures of interest. The experiment is designed to capture a large field of view with good resolution; 55,400 vectors over a spanwise length exceeding 3 δ and a streamwise length exceeding 2.5 δ permit observations of large-scale phenomenon while adequately resolving the individual structures within these motions.

The measurements reveal low momentum regions elongated in the streamwise direction that are consistent with the earlier work in the streamwise-wall-normal (x-y) plane. Velocity vector patterns are consistent with the idea that vortex packets induce these low-speed regions, as rotating/swirling patterns typically occur on the borders of these large-scale motions. Packets are observed with as many as 9 vortex members. Inspection of individual vortex structures occasionally reveals symmetry about the x-y plane, though more frequently these appear to be asymmetric; both are consistent with the hairpin vortex interpretation. The streamwise extent of these low momentum regions ranges up to and beyond 2 δ, completely consistent with the earlier results; their spanwise extent typically ranges from 0.2 to 0.4 δ. The intersection of the measurement volume with these low-momentum regions takes on a variety of shapes, the dominant one being an elongated elliptical or rounded rectangle, although wedge-shaped regions and wider patterns do exist. There exists a typical range of center-to-center spacing between these large-scale motions, centered around 0.8 δ or so, corresponding to over 1700 viscous wall units.

EXPERIMENT

Wind Tunnel Facility

Measurements are performed in a low-turbulence open circuit Eiffel type wind tunnel. Air is drawn in through an elliptical inlet, travels through a series of screens and honeycomb, and is accelerated into the test section through a contraction ratio of 10:1. Zero pressure gradient is obtained by adjusting the height of the roof of the tunnel. The boundary layer plate is flat, smooth, and 6096 mm long by 914 mm wide; this width is approximately 10 times the boundary layer thickness in this study, so side effects were minimal. A 4.7 mm diameter circular rod was placed flat on the test section to trip the boundary layer at $x = 110$ mm. The center of the measurement volume is located at 5310 mm from the leading edge, at a height of $y/\delta = 0.2$. A more complete description of the wind tunnel, as well as an evaluation of performance, is given in Meinhart (1994). He estimated the free-stream turbulence intensity throughout a cross section at $x = 650$ mm to be 0.16%.

TABLE 1: FLOW PARAMETERS

Re_θ ($U_\infty\theta/\nu$)	7700
U_∞ (m/s)	11.4
θ (mm)	10.35
u_τ (m/s)	0.41
y^* (mm)	0.038
δ (mm)	83.1
δ^+	2200

Flow Parameters

The turbulent boundary layer has an approximate Reynolds number of $Re_\theta = U_\infty\theta/\nu \approx 7700$, where U_∞ is the free stream velocity, θ is the momentum thickness, and ν is the kinematic viscosity. The experiment was designed to match the high Reynolds number case of Tomkins (1997) for comparison. This was done by matching all controllable parameters; error in Re_θ between the two experiments may be as great as 2% due to differences in atmospheric pressure. The average streamwise velocity is computed for the current data by ensemble averaging all realizations and then area averaging the result; this is compared with that obtained in the x-y results at the same wall-normal location, $y/\delta = 0.2$. The results differ by only 3%, within the sampling error for these experiments. Table 1 shows several relevant flow parameters calculated from the x-y experiment. Momentum thickness θ is estimated by numerically integrating the boundary layer profile. Wall friction velocity u_τ is estimated using the chart method of Clauser (1956), and the boundary layer thickness δ is calculated using the 0.99 criterion.

PIV Measurements

Particle image velocimetry is used to obtain instantaneous 2-dimensional velocity fields in the streamwise-spanwise (x-z) plane (Adrian, 1991). Measurements are performed at a wall-normal distance of $y/\delta = 0.2$, corresponding to $y^+ \approx 440$. This plane is specifically chosen to compliment the x-y results; the light sheet will directly intersect the large-scale motions of immediate interest. Optical access is gained through large glass windows on the sides of the test section and a float glass piece set into the boundary layer plate. Two Continuum Nd:YAG lasers each produce about 200 mJ of light @ $\lambda = 532$ nm in under 10 ns, illuminating olive oil droplets of nominal diameter 1-2 μm. The lasers are spread out into a wide 250 mm sheet using a series of negative cylindrical lenses, and focused down to a minimum thickness in the test section center using a positive cylindrical lens. The lasers are timed using a Stanford timing box, and here pulse separation was set at 44 μs to achieve a displacement/particle image size ratio around 4. The light sheets are set at $y = 16.6$ mm, using alignment blocks with machined slots to guarantee accurate height over the whole measurement area. The light sheets cut through the test section in the spanwise direction, scattering light through the float glass plate in the test section floor to a 45 degree angled mirror, which reflects the particle images upstream to a film camera. The camera uses an enlarging lens optimized for large magnifications installed backwards to achieve minimal

TABLE 2: MEASUREMENT PARAMETERS

y/δ	0.2
y^+	440
Field of view, x	2.5 δ
Field of view, z	3 δ
# of Vectors	55,400
Δx^+	26.5
Δz^+	26.5
Δy^+	10.0

distortions with a wide field of view. The recording medium is large-format 4" by 5" T-MAX 400 photographic film. These components are designed to obtain a large field of view; the interrogated area extends over 3 δ spanwise and over 2.5 δ streamwise.

With this system a total of 46 realizations are captured. The data is interrogated by back illuminating individual negatives with incoherent light, then scanning the whole area section-by-section using a Videk Megaplus 1024 x 1024 CCD camera and processing individual sections. Sections are interrogated using a single-frame, double-exposure, cross-correlation algorithm running on a Dell 266 MHz PC with dual processors. Raw velocity information is then post-processed, with invalid measurements being removed (Meinhart, 1994; Soloff, 1998). Missing vectors due to removal can be replaced with alternate vectors corresponding to other peaks in the correlation plane during interrogation, or from interpolation if the percentage of neighboring valid measurements is high for a given location. A Gaussian low-pass filter is then used to remove noise present in the vector field.

The resulting vector fields contain a low percentage of obviously bad vectors with an interrogation spot size corresponding to 1.99 mm per side in physical space. With 50% overlap between neighboring interrogation spots, this results in a spatial resolution of 0.99 mm per side, or 26.5 inner units in the spanwise and streamwise directions. The light sheet thickness defines the resolution in the wall-normal direction, with $\Delta y^+ = 10$. In such a flow, this spatial resolution is insufficient to properly resolve all of the scales of the flow. However, it is sufficient to observe the structures of immediate interest. Furthermore, because this resolution is achieved over such a large area, it produces enough information (over 55,400 vectors) to allow simultaneous observation of the large-scale motions associated with these individual structures. These figures are listed along with other measurement parameters in Table 2.

INSTANTANEOUS FIELDS

Large-scale Low Momentum Structures

The most commonly occurring flow structures at this wall-normal location and Reynolds number are large-scale low momentum regions elongated in the streamwise direction. Two or more of these structures appear in nearly every realization. Contours of constant streamwise velocity are shown in Figure 1 for three independent sample realizations.

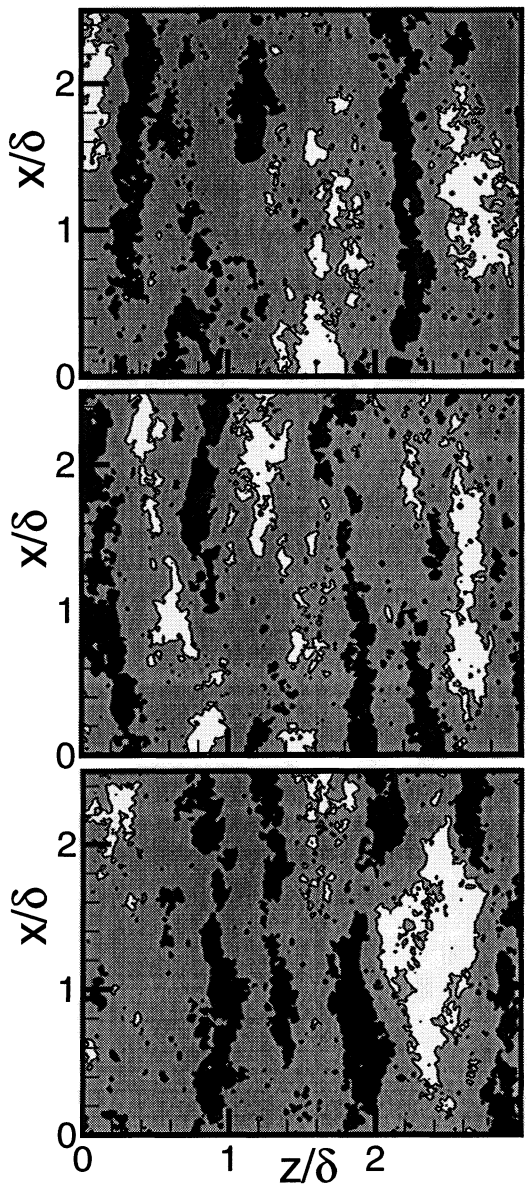

Figure 1. Contours of constant streamwise velocity in x-z plane at 0.65 U_∞ (dark) and 0.85 U_∞ (light). $U_{avg} = 0.75\ U_\infty$.

Contours are set at 0.65 U_∞ and 0.85 U_∞, while the mean velocity here is 0.75 U_∞. The axes have been normalized by the boundary layer thickness, and the flow is from bottom to top. The channel center is at x/δ= 1.62. Light regions represent high momentum fluid, and dark regions represent low momentum fluid. All three realizations show elongated dark regions, representing large-scale low momentum structures in the fluid. These structures are not the well-documented low speed streaks; rather, they extend well into the boundary layer (here $y^+ = 440$). The streamwise extent of these structures can exceed 2 δ, as is the case with certain examples in Figure 1.

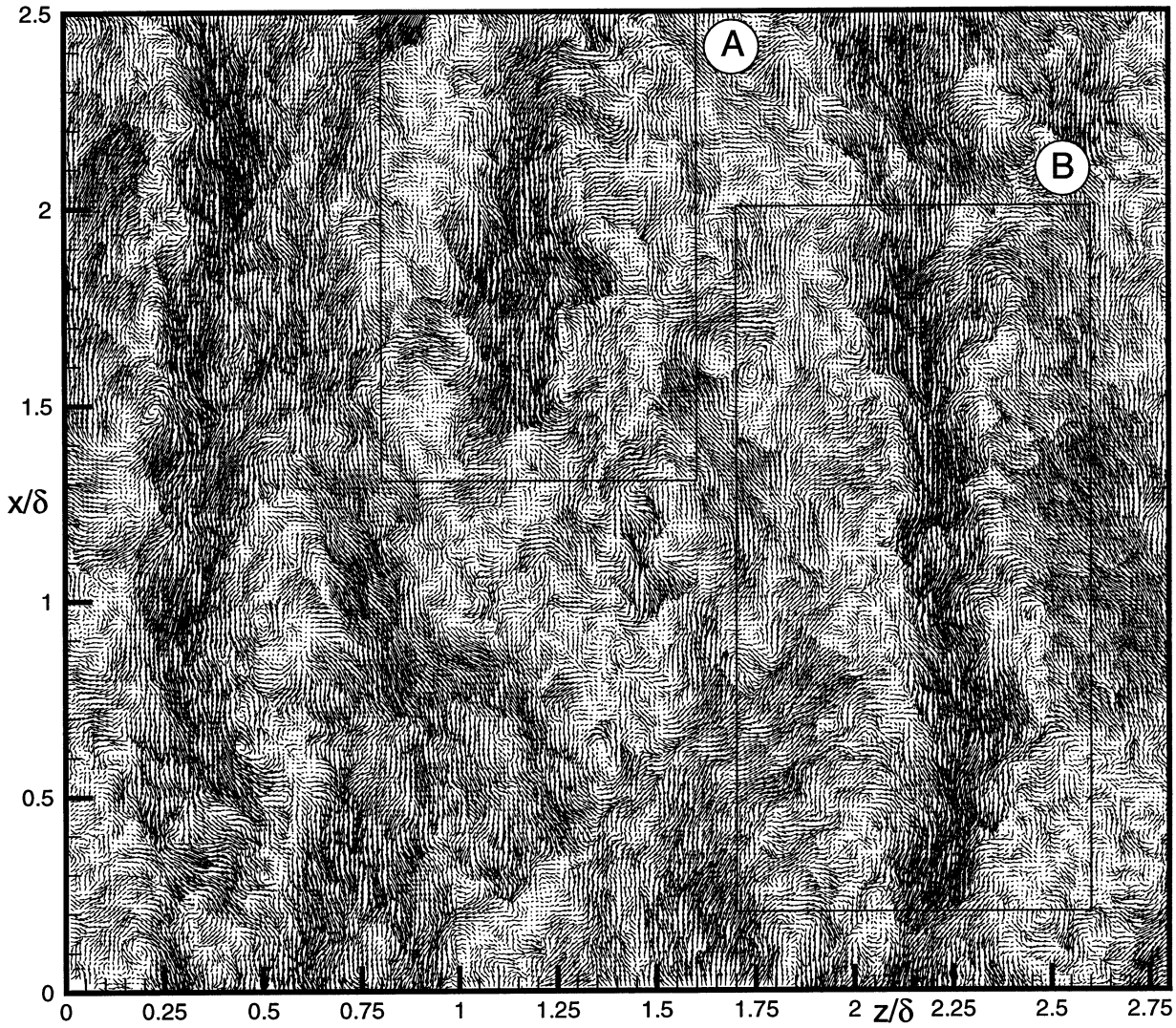

Figure 2. Instantaneous fluctuating velocity vectors in the x-z plane at $y/\delta = 0.2$ with $U_c = 0.88\ U_\infty$.

In terms of viscous wall units this corresponds to an enormous length, over 4400. These figures are completely consistent with the *x-y* plane results previously discussed (Meinhart et al. 1999) etc. in which inclined low momentum regions grow upwards from the wall. The spanwise extent of these structures is typically 0.2 - 0.4 δ and the examples shown here fall within this range. This corresponds to a range of $z^+ = 440\text{-}880$, so several low speed streaks may exist along the wall underneath each of these structures. The shape of these structures varies. The examples here are typical and represent the most commonly observed patterns; however, thicker wedge-shaped or diamond-shaped patterns are also seen. Spanwise spacing of these structures is estimated to be in the range 0.5 to 1.2 δ, centered around 0.8 δ.

Association with Vortex Packets

Plots of instantaneous velocity vectors confirm the existence of structures observed in the streamwise velocity contour plots, and provide greater insight into their nature. Figure 2 shows instantaneous velocity vectors for the uppermost example in Figure 1 in the range $0 < z/\delta < 2.8$. In viewing these vector plots one decomposes the velocity field into mean and fluctuating parts. With Reynolds decomposition one subtracts a constant equal to the mean velocity at that wall-normal position, as the flow is homogeneous in the mean in the streamwise and spanwise directions. The fluctuating field then appears as though one is moving with the fluid at that mean velocity. It is clear from Figure 2 chunks of fluid are moving at different speeds; one may also choose to move with several of these by changing the convection constant. The constant in Figure 2 is just slightly greater than the mean, $U_c = 0.77\ U_\infty$. Cursory inspection reveals large regions of low

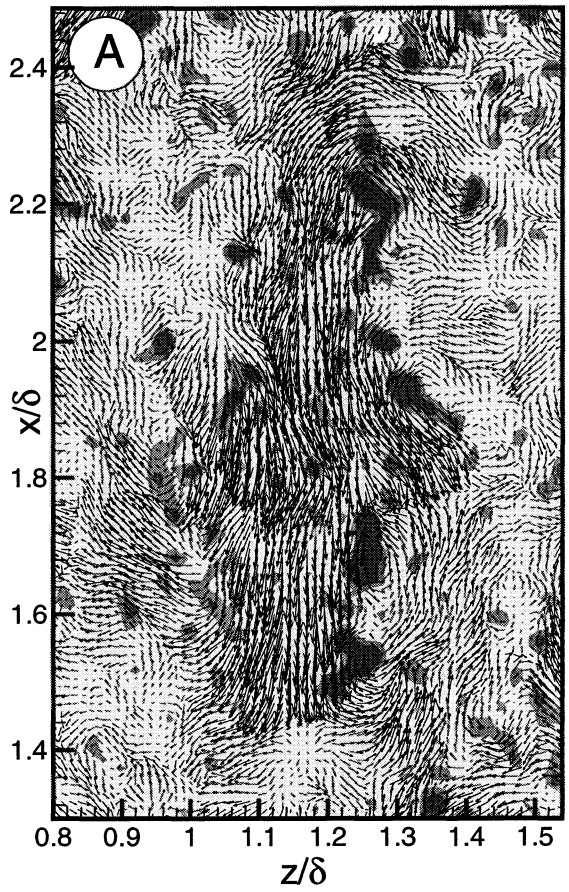

Figure 3. Velocity vectors with vorticity for extracted Region A in Figure 2.

momentum fluid in correspondence with the velocity contours. Close inspection reveals a series of swirling, vortex-like motions lining the borders of these structures. These patterns are consistent with the idea that inclined hairpin-like vortex structures are intersecting the measurement volume, and the inclined counter-rotating legs of these structures appear as counter-rotating elliptical swirling motions. In the hairpin packet paradigm, these structures are individual hairpin vortex-like members of vortex packets, and have aligned in the streamwise direction through generation and/or organization. These structures work cooperatively to induce the low momentum fluid between (hairpin vortices) or alongside (cane-like vortices) their legs and underneath their heads, passing low-speed fluid backwards in a relative sense as they propagate downstream with little dispersion. In order to more rigorously test this concept against the present data, two of these large-scale structures are extracted and examined more closely.

Figures 3 and 4 show the velocity vectors plotted with contours of magnitude of vorticity for the two extracted regions, labeled A and B in Figure 2, respectively. Again the axes are normalized by δ, and a constant convection velocity is subtracted, in this case the mean velocity

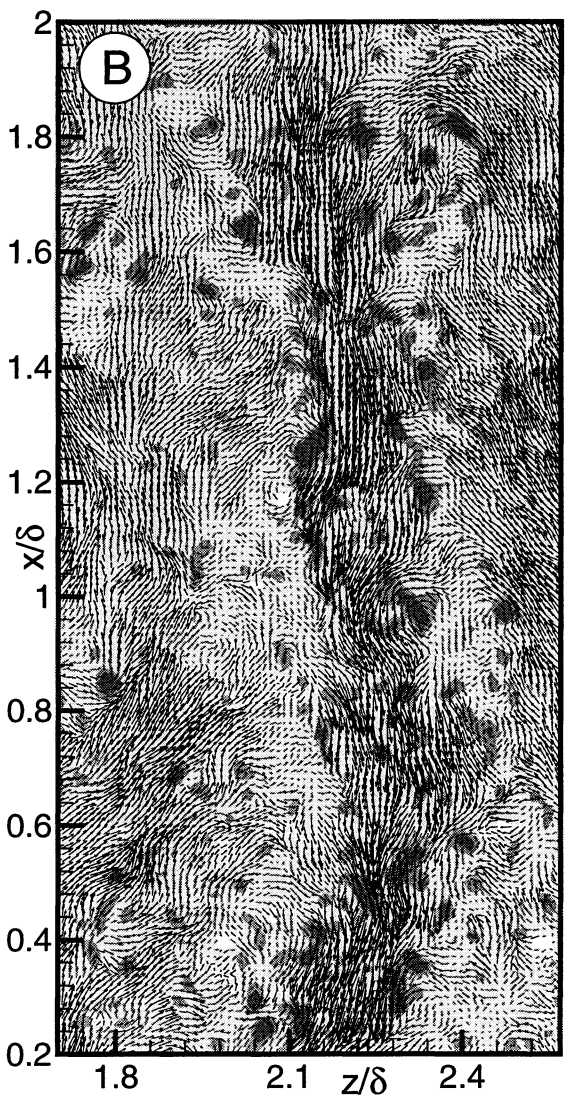

Figure 4. Velocity vectors with vorticity for extracted Region B in Figure 2.

(Reynolds decomposition). Magnitude of vorticity is used for this black and white plot; typically the vorticity on either sides of these structures is opposite in sign. Both Figures reveal the low-momentum regions are bordered by regions of relatively high vorticity levels, with relatively low occurrence of such vorticity in the surrounding fluid. Inspection also reveals swirling motions surrounding these vorticity peaks, rotating in the direction with the low momentum region. These observations suggest the large scale low-speed structures may be induced by a series of vortices, in exact agreement with the hairpin packet paradigm. Examination of individual structures (members of packets in the packet interpretation) commonly reveals one-sided asymmetric vortex structures (cane-like) or two-sided asymmetric vortex structures (hairpin-like), and less commonly two-sided symmetric structures (hairpin-like). All three patterns are wholly

consistent with the hairpin packet concept. The individual structures are indeed aligned in the streamwise direction, although some waviness occurs along the streamwise direction. This waviness is typically on a larger scale than the individual vortex spacing. Vorticity plots suggest these large scale motions have roughly 4-6 (Figure 3) and 7-9 (Figure 4) associated vortices. These numbers are typical, as are the large-scale structures.

CONCLUSIONS

PIV is used to obtain instantaneous wide field of view velocity fields in the streamwise-spanwise plane of a $Re_\theta \approx$ 7700 turbulent boundary layer at $y/\delta = 0.2$. The dominant flow structure observed is a large-scale low momentum region elongated in the streamwise direction; this structure is consistent with observations of low-momentum ramps angling upwards from the wall in *x-y* plane data, and distinct from the near-wall low speed streaks. Regions of high opposite-sign vorticity and rotating velocity vector patterns consistently border these large-scale motions, suggesting they are induced by packets of inclined hairpin-like vortices aligned in the streamwise direction.

These large-scale structures may extend over 2 δ streamwise, and typically have a spanwise width in the range $\Delta z = 0.2 - 0.4\ \delta$, resulting in a length to width ratio ranging from about 1.5 to 10. The shapes created by the intersection of the light sheet with these structures vary greatly; they include rectangles of roughly uniform spanwise thickness with rounded edges (most common), slightly angled diamonds or wedges, and thick wedges with corrugated edges. The large-scale low momentum regions themselves may organize or interact in the spanwise direction. Spacing between motions at this wall-normal location is observed in a range between 0.5 and 1.2 δ, centered around 0.8 δ, which corresponds to over 1700 viscous wall units.

Close inspection of large-scale motions reveals fluctuating velocity vector patterns and vorticity peaks suggesting the presence of inclined hairpin-like vortices. Cane-like and asymmetric hairpin-like structures are most commonly observed, although symmetric hairpin-like structures appear as well; all three patterns fit within the context of the hairpin packet paradigm. The vortices consistently align in the streamwise direction, although slight waviness is sometimes present on a length scale several times larger than the individual vortex spacing. In the hairpin vortex packet interpretation, these large-scale motions (vortex packets) typically contain 4-9 individual vortex members.

ACKNOWLEDGEMENTS

This work was supported in part by ONR N0001-97-1-01091. A special thanks to Ken Christensen for modifying an existing HPIV interrogation system for film.

REFERENCES

Adrian, R. J., 1991, "Particle-imaging Techniques for Experimental Fluid Mechanics," *Ann. Rev. Fluid Mech.*, Vol. 23, pp. 261-304.

Clauser, F., 1956, "The Turbulent Boundary Layer," *Advances in Applied Mechanics*, Vol. 4, pp. 1-51.

Head, M. R., and Bandyopadhyay, P., 1981, "New Aspects of Turbulent Boundary Layer Structure," *J. Fluid Mech.*, Vol. 107, pp.297-338.

Kline, S. J., Reynolds, W. C., Schraub, F. A., and Runstadler, P. W., 1967, "The Structure of Turbulent Boundary Layers," *J. Fluid Mech.*, Vol. 30, part 4, pp. 741-773.

Liu, Z.-C., Adrian, R. J., Hanratty, T. J., 1996, "A Study of Streaky Structures in a Turbulent Channel Flow with Particle Image Velocimetry," *Proceedings, 8th International Symp. on Appl. of Laser Techn. to Fluid Mech.*, Lisbon, Portugal.

Meinhart, C. D., 1984, "Investigation of Turbulent Boundary Layer Structure Using Particle-image Velocimetry," Ph.D. Thesis, University of Illinois at Urbana-Champaign, Urbana, IL.

Meinhart, C. D., and Adrian, R. J., 1996, "On the Existence of Uniform Momentum Zones in a Turbulent Boundary Layer," *Phys. Fluids*, Vol. 7, pp. 694-696.

Meinhart, C. D., Adrian, R. J., and Tomkins, C. D., 1999, "Vortex Organization in the Outer Region of a Turbulent Boundary Layer," (manuscript in preparation).

Smith, C. R., 1984, "A Synthesized Model of the Near-wall Behavior in Turbulent Boundary Layers", *Proceedings, 8th Symp. On Turbulence*, G. K. Patterson and J. K. Zakin, ed., University of Missouri-Rolla, Dept. of Chemical Engineering, Rolla, Missouri.

Soloff, S. M., 1998, "An Investigation of the Small-scale Structure in a Turbulent Pipe Flow Using High Resolution Particle Image Velocimetry," M. S. Thesis, University of Illinois at Urbana-Champaign, Urbana, IL.

Tomkins, C. D., 1997, "A Particle-image Velocimetry Study of Coherent Structures in a Turbulent Boundary Layer," M. S. Thesis, University of Illinois at Urbana-Champaign, Urbana, IL.

Tomkins, C. D., Adrian, R. J., and Balachandar, S., 1998, "The Structure of Vortex Packets in Wall Turbulence," AIAA Paper No. 98-2962.